



ELSEVIER

Journal of Alloys and Compounds 330–332 (2002) 241–245

Journal of  
ALLOYS  
AND COMPOUNDS

www.elsevier.com/locate/jallcom

# Evolution of microstructure in the $\text{LaNi}_5\text{-D}$ system during the early absorption–desorption cycles

M.P. Pitt<sup>a</sup>, E. MacA. Gray<sup>a,\*</sup>, B.A. Hunter<sup>b</sup><sup>a</sup>School of Science, Griffith University, Brisbane 4111, Australia<sup>b</sup>Neutron Scattering Group, Australian Nuclear Science and Technology Organisation, Locked Bag 1, Menai 2234, Australia

## Abstract

During the first few hydrogenation–dehydrogenation cycles of virgin  $\text{LaNi}_5$ , the absorption plateau pressure drops sharply, accompanied by powdering of the starting intermetallic. We looked for an explanation of this phenomenon in the microstructural features of the metal that can be studied via diffraction. Five complete absorption–desorption cycles were conducted in an unbroken sequence, with neutron powder diffraction patterns being recorded in cycles 1, 2 and 5. We found that, after activation, the drop in absorption plateau pressure correlates with increasing coherency of the phase transformation in the  $c$ -direction, translating to lower elastic strain energy associated with the transformation. The total microstrain in the dehydrogenated metal is essentially constant after cycle 1. These findings afford a partial understanding of the pressure behaviour in the first few cycles, but the mechanism by which the lattice coherency develops remains to be explained. © 2002 Elsevier Science B.V. All rights reserved.

**Keywords:** Metal hydrogen; Activation; Neutron diffraction; Strain; Dislocation

## 1. Introduction

Our previous study [1] of the activation process in  $\text{LaNi}_5$  by in-situ neutron powder diffraction provided a fairly clear physical picture of the activation mechanism which operates during the first absorption. The host matrix initially absorbs hydrogen to the point of saturation of the  $\alpha$  phase.  $\beta$  nuclei then form and physically separate from the parent particles because the misfit strain cannot be supported by the  $\alpha$  phase in the virgin (i.e. unactivated) intermetallic.

Within the course of the first few hydrogenation–dehydrogenation cycles, the hydrogen absorption properties of the  $\text{LaNi}_5\text{-H}_x$  system acquire characteristics that may persist for thousands of cycles, changing slowly as the host alloy gradually degrades [2]. The activation period is characterised by a reduction in physical grain size (powdering) and the introduction into the newly formed  $\beta$  phase of dislocations of the type  $\frac{a}{3}\langle 2110 \rangle\{0110\}$ , revealed in severe anisotropic diffraction line broadening [3–6]. This establishes a microstructure which persists in the dehydrogenated metal thereafter. Starting with the first desorption and continuing through subsequent cycles, nanoscopic mechanical interaction between the phases is revealed by

lattice parameters that depend on the phase proportions [1,7]. This co-existence is apparently made possible by the existence of a very high density of dislocations in material that has previously absorbed hydrogen.

Macroscopically, a large reduction in absorption plateau pressure is observed between cycles 1 and 2, continuing in smaller steps, until by cycle 5 it can be considered to be stable. In contrast, the desorption plateau pressure changes only slightly between cycles 1 and 5. Recent work by Inui et al. [8] shows that the initial decrease in absorption pressure is caused by cracking of the virgin metal particles.

The aim of this study was to observe any distinctive microstructural changes in the first few hydrogenation cycles, and if possible, to correlate them with the well-known changes in the hydrogenation behaviour.

## 2. Experimental details

The sample studied was closely stoichiometric  $\text{LaNi}_5$  (Santoku). A 32-g sample was ground in air, sieved to 53–106  $\mu\text{m}$ , and quickly transferred to an aluminium sample can. The sample was evacuated with a turbopump and heated to 80°C for several hours to desorb surface impurities. It was stored under vacuum until the neutron diffraction experiment, which was conducted at 40°C. This

\*Corresponding author.

study was performed using the diffractometer HRPD ( $U=0.05792^\circ$ ,  $V=-0.15000^\circ$ ,  $W=0.14000^\circ$ ) at the reactor HIFAR, operated by the Australian Nuclear Science and Technology Organisation, Sydney. Data were collected in the range  $10\text{--}154^\circ$  ( $2\theta$ ) in  $0.05^\circ$  increments at  $\lambda=1.8823$  Å. A total of 32 diffraction patterns were recorded during cycles 1, 2 and 5, at pressures up to 42 bar. Typically, single-phase patterns were accumulated for 12 h and two-phase patterns were accumulated for 24 h. The entire experiment was performed in situ, in a single sequence, using ultra-pure deuterium desorbed from a  $\text{LaNi}_5$  storage bed. Changes in deuterium-to-metal atomic ratio,  $D/M$ , were measured throughout the experiment by the manometric technique described in Ref. [1]. This allowed us to confirm that the change in  $D/M$  while a pattern was recorded was always small compared to the absolute  $D/M$ .

### 3. Results and analysis

The Rietveld code LHPM was used to analyse the diffraction patterns with a generic basal plane  $\Delta a/a$  strain model [7]. In this model, the anisotropic strain broadening is ascribed to a basal-plane stretch  $\Delta a$  which is included in the overall Gaussian contribution to the peak breadth  $U$  according to

$$U(2\theta) = U_1 + \left[ \frac{2(h^2 + hk + k^2)/a^2}{(h^2 + hk + k^2)/a^2 + \frac{3}{4}(\frac{l^2}{c^2})} \cdot \frac{\Delta a}{a} \right]^2$$

where  $U_1$  is the instrumental contribution. Although simple, this model emulates exactly the functional dependence of the Gaussian breadth owing to  $\frac{a}{3}\langle 2110 \rangle\{0\bar{1}10\}$  dislocations [5].

Fig. 1 shows a typical two-phase refinement of the diffraction pattern recorded in the centre of the desorption plateau of cycle 2. The  $\alpha$  phase was modelled in space group  $P6/mmm$ , and the  $\beta$  phase in  $P31c$ . The latter space group, used with a doubled  $c$ -axis relative to  $P6/mmm$ , models the D ordering whose occurrence is visually indicated by the appearance of the (023) superlattice peak once the pure  $\beta$  phase is entered at the end of the absorption plateau [9]. The agreement index  $R_B$  ranged from 0.8 to 2.5% for all fits, while the GOF varied from 1.7 to 2.8. Systematic problems were encountered in using the split-site multi cell  $\beta$  model, leading to high values of the GOF. The cause was the interplay of isotropic broadening and the Ni 2b thermal parameters, in the filling of the mixed D site 6c, and in the emptying of one half of the split D site 2b. It was necessary to account for isotropic broadening because it contains components of size, dislocation and interfacial strain broadening [4,5]. The stability of the refinements was rather sensitive to the magnitude of the isotropic broadening parameter, which in turn is critical

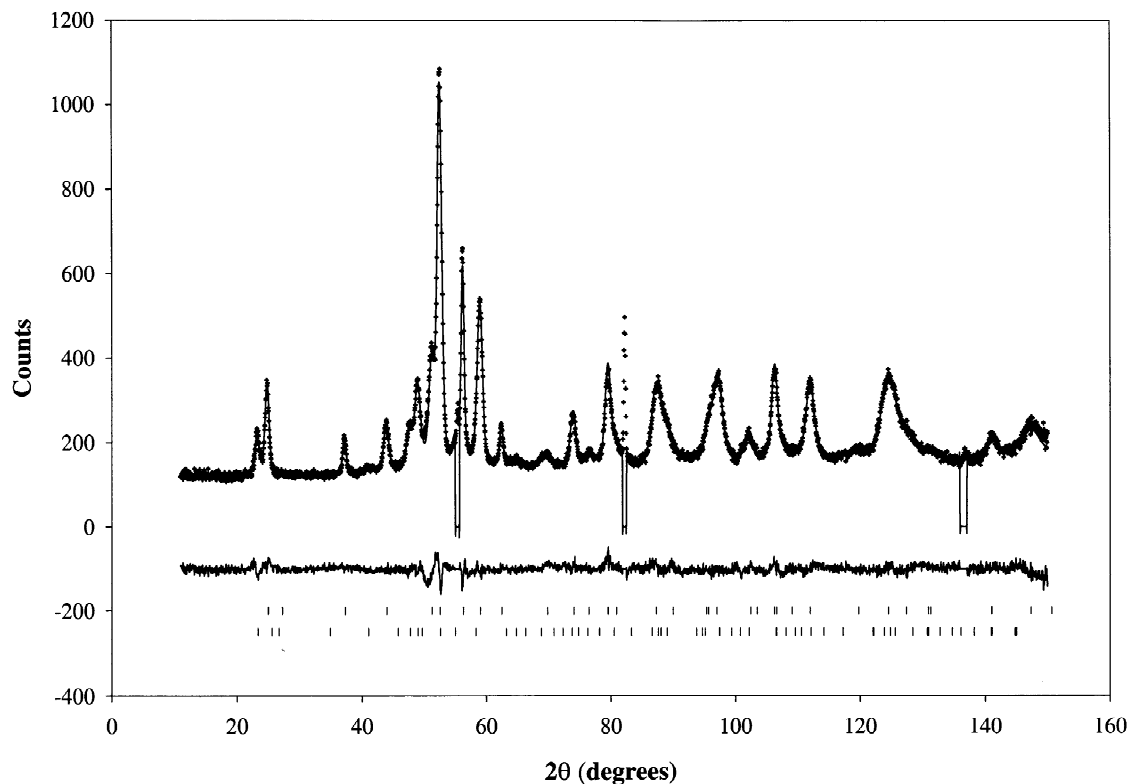


Fig. 1. Typical two-phase diffraction pattern recorded at  $D/M=0.35$  (determined by quantitative phase analysis) in desorption. The measured pattern is indicated by points, the fitted pattern and difference pattern (below) by lines. The reflection markers are for the  $\alpha$  (upper set) and  $\beta$  (lower set) phases. The excluded regions correspond to peaks from the Al pressure chamber.

to the fit of (002). Attempts to vary the metal thermal parameters in the  $\beta$  structural model in two-phase fits resulted in excessively high values, and in nearly all cases, the isotropic broadening would change sign and lead to unstable refinements. This interplay could not be directly observed in the correlation matrix. For this reason, all  $\beta$  metal thermal parameters were refined from single-phase fits close to the phase boundary, and subsequently fixed in two-phase fits. Further, the D site occupancies in the  $\beta$  structural model were refined from a pattern in the centre of each isotherm and fixed in multiple phase patterns along the rest of each isotherm. This methodology allows for the subsequent use of the lever rule for quantitative phase analysis (QPA). This approach to two-phase refinements proved to be the most stable. In all cases, the agreement between D content as extracted from the diffraction data and as measured directly was excellent.

Fig. 2 shows the evolution of the  $c$  lattice parameter of each phase during cycle 2. Also included for comparison are the values of  $c_\beta$  in absorption for cycles 1 and 5. Comparing the lattice parameter variation with D concentration between cycles 1, 2 and 5 led to the following observations:

- These data agree very well with our previous measurements during cycle 1 [1].
- After the first absorption (activation) [1],  $a$  for both phases changes little.
- Likewise  $c_\alpha$  changes relatively little after the very first absorption of hydrogen.
- The changes in  $c_\beta$  during desorption from cycles 1 to 5 are not significant within the level of uncertainty.
- Striking changes do occur, however, in  $c_\beta$  during absorption. While its value in the pure  $\beta$  phase is stable,  $c_\beta$  decreases significantly between cycles 2 and 5 at low concentration, where the  $\beta$  phase is nucleating in the  $\alpha$  matrix. This implies an increasing degree of coherency between the  $\alpha$  and  $\beta$  phases during  $\beta$  nucleation as the cycle number increases.

Fig. 3 shows the variation in total anisotropic microstrain for cycle 2, as measured with the generic basal-plane  $\Delta a/a$  strain model. Also shown for comparison are the data for desorption in cycle 1. The strain results can be summarised as follows:

- Aside from the activation half-cycle, the strain in the  $\alpha$  phase is essentially stable from cycle to cycle, although the variation with changing H concentration is large.
- The strain in the  $\alpha$  phase is highest in the pure-phase region.
- In absorption, the strain in the  $\beta$  phase varies little with  $D/M$ , and appears stable within uncertainty after cycle 2, although significantly higher than in cycle 1.
- In desorption, however, the behaviour of the strain parameter for the  $\beta$  phase is essentially the same

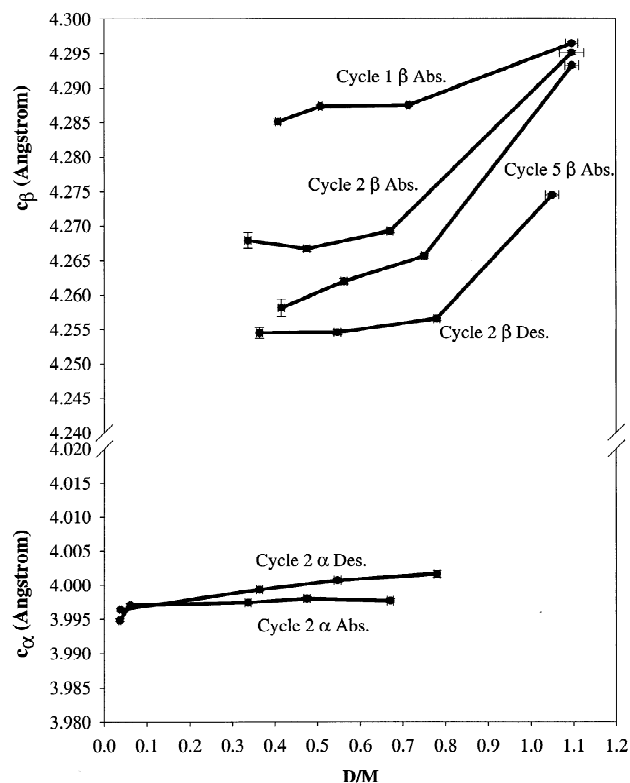


Fig. 2. Variation of the  $c$  lattice parameter of the  $\alpha$  and  $\beta$  phases with  $D/M$  in cycle 2, referred to the  $P6/mmm$  cell of the  $\alpha$  phase. Also shown is  $c_\beta$  during absorption in cycles 1 and 5. Notice that, while its value in the pure  $\beta$  phase is stable,  $c_\beta$  decreases significantly between cycles 2 and 5.

between cycles 2 and 5, but significantly different from cycle 1.

Fig. 4 shows the variation with  $D/M$  of the notional particle size, which is the coherently diffracting domain size calculated from the Lorentzian breadth of the diffraction peaks, assuming spherical domains. Strict physical interpretation of this parameter is unwise, but its behaviour is interesting. Data are shown only for cycle 2 because, with the exception of the  $\alpha$  phase during cycle 1 absorption (activation), very much the same results were obtained in cycles 1 and 5. Whereas the domain sizes in Fig. 4 are a few hundreds of angstrom, the domain size of the  $\alpha$  phase during activation was approximately constant at  $2200 \text{ \AA} \pm 10\%$  throughout the course of the absorption isotherm.

#### 4. Discussion

The foregoing microscopic observations need to be examined in relation to the sharp fall in the absorption pressure, and the relative constancy of the desorption pressure, during the first few hydrogenation cycles. The data must be interpreted with caution because powder diffraction is an averaging technique. Furthermore, phys-

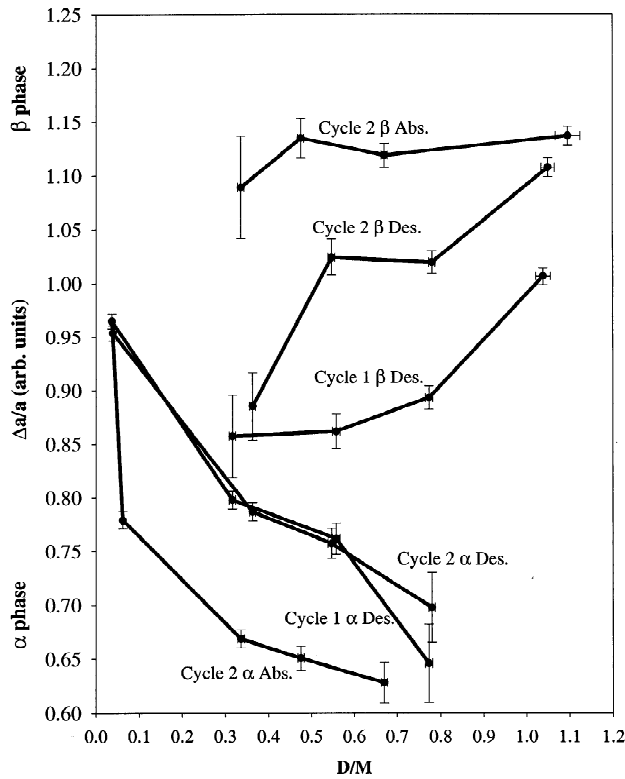


Fig. 3. Variation of the total anisotropic microstrain, expressed as  $\Delta a/a$ , for cycle 2. Also shown are the data for desorption during cycle 1.

ical interpretation is based on the assignment to physical origins of features of the diffraction peaks, especially their shape and breadth. For instance, it is known that dislocations contribute a Lorentzian peak shape component as well a Gaussian one [4,5], and this will be modelled by other breadth-related parameters in this analysis. This is especially true in the two-phase region, where interfacial strain and dislocation strain are convolved in the data.

The following generic picture is commensurate with the experimental data known to us and is used as a framework for discussion. During the activation process, a grain structure is developed in the hydrided metal. The coherently diffracting domains are bounded by wall-like structures, no doubt built from dislocations, which are stable and constitute a microstructural memory of the activation process. As the  $\beta$  phase nucleates in the  $\alpha$  phase, or vice versa, each of these domains is converted to the other phase, perhaps immediately or perhaps, since the generation of energy-consuming misfit dislocations is involved, gradually as the pressure rises. In either case, interfacial strain between the phases occurs directly, or indirectly, transmitted by the domain wall.

The ease of accommodating the interfacial strain between the  $\alpha$  and  $\beta$  phases must play a role in the determination of the absorption and desorption pressures. That there appears to be higher lattice coherency in the  $c$ -direction than in the basal plane is of course consistent with the accommodation of basal-plane strain in the

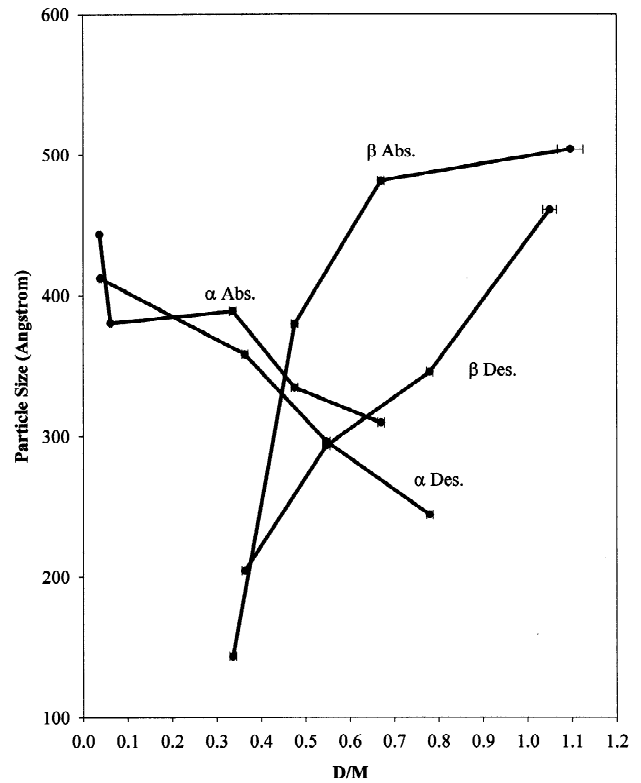


Fig. 4. Variation of the notional particle size with  $D/M$  for cycle 2. Cycle 1 (desorption) and cycle 5 are essentially the same. Note the trends to smaller particle size in the  $\alpha$  phase and larger size in the  $\beta$  phase as the  $\alpha$ - $\beta$  transformation proceeds.

$\frac{a}{3}\langle 2110\rangle\{01\bar{1}0\}$  misfit dislocations observed. The decreasing value of  $c_\beta$  in absorption as we progressed from cycle 1 to cycle 5 is expected to lower the compressive strain energy stored in  $\beta$  phase nuclei, which should be manifest as a lower absorption pressure through its lower energy cost. This is consistent with the macroscopic behaviour of the system.

The reason why  $c$ -coherency might increase with cycling is unclear. The  $\beta$  phase is evidently softer in the  $c$ -direction than the  $\alpha$  phase, as evidenced by the much greater variation of  $c_\beta$ , but the origin of the effect remains unexplained. An increasing dislocation density does not appear to be the cause because the strain in the pure  $\alpha$  phase is remarkably stable from cycle to cycle.

One clear feature of the data is the behaviour of the notional particle size. The decrease in particle size owing to activation, and its subsequently stable behaviour, are consistent with the finding of Inui et al. [8] that the initial pressure drop is caused by cracking. Post activation, Fig. 4 shows that the particle size in the pure  $\alpha$  phase is the same as in the pure  $\beta$  phase within the uncertainty with which it can be determined. Furthermore, the  $\alpha$  size decreases and the  $\beta$  size increases as the  $\alpha$ - $\beta$  phase transformation proceeds and vice versa. When the sample is in the form of pure  $\alpha$  or  $\beta$  phase, the diffraction pattern is due to coherently diffracting domains whose size is generally

called the particle size. Suppose that a domain can transform from pure  $\alpha$  to pure  $\beta$  and back while retaining its basic structural coherency. The behaviour of the particle sizes for the  $\alpha$  and  $\beta$  phases then suggests that the phase transformation within each coherently diffracting domain proceeds gradually and that, in the two phase region, each domain contains both the  $\alpha$  and the  $\beta$  phase. Therefore the nanoscopic mechanical interaction between phases indicated by the dependence of lattice parameters on phase proportions appears to arise at (from the diffraction point of view) the most fundamental level. This interpretation relies on the assignment of the Lorentzian contribution to the diffraction peaks to particle size broadening. As the functional dependence ( $\sec \theta$ ) differs from that for dislocation broadening ( $\tan \theta$ ), it is a reasonable interpretation, being based on whole-pattern fits to the data.

## 5. Conclusions

An in-situ neutron diffraction study of the  $\text{LaNi}_5\text{-D}$  system during hydrogenation cycles 1, 2 and 5 has given some insight into how the microstructure of this metal-H system develops. The key question is that of how the microstructure determines the absorption pressure.

No substantial change in the residual strain owing to dislocations was observed from cycle to cycle; the dislocation structure appears to be established during the very first absorption by virgin metal, and to be stable thereafter. Our data suggest that the degree of coherency between the  $\alpha$  and  $\beta$  phases in the  $c$ -direction plays a role in controlling the plateau pressures via the contribution to hysteresis of elastic strain energy, although the mechanism is not yet clear.

Our data support a picture of the  $\alpha$ - $\beta$  phase transformation in which these phases co-exist in every coherently diffracting (when single-phase) domain.

## Acknowledgements

This work was supported by the Australian Institute of Nuclear Science and Engineering. The help of Dr Erich Kisi, University of Newcastle, and of Dr Shane Kennedy at ANSTO, is gratefully recognised. EMG thanks Professor Etsuo Akiba for providing the  $\text{LaNi}_5$ .

## References

- [1] M.P. Pitt, E.MacA. Gray, E.H. Kisi, B.A. Hunter, *J. Alloys Comp.* 293–295 (1999) 118–123.
- [2] E.MacA. Gray, T.P. Blach, C.E. Buckley, *J. Alloys Comp.* 293–295 (1999) 57–61.
- [3] G.H. Kim, S.G. Lee, K.Y. Lee, C.H. Chun, J.Y. Lee, *Acta Metall. Mater.* 43 (1995) 2233–2239.
- [4] E. Wu, E.MacA. Gray, E.H. Kisi, *J. Appl. Crystallogr.* 31 (1998) 356–362.
- [5] E. Wu, E.H. Kisi, E.MacA. Gray, *J. Appl. Crystallogr.* 31 (1998) 363–368.
- [6] R. Cerny, J.-M. Joubert, M. Latroche, A. Pecheron-Guegan, K. Yvon, *J. Appl. Crystallogr.* 33 (2000) 997–1005.
- [7] E.H. Kisi, E.MacA. Gray, S.J. Kennedy, *J. Alloys Comp.* 216 (1994) 123–129.
- [8] H. Inui, T. Yamamoto, M. Hirota, M. Yamaguchi, *J. Alloys Comp.* 330–332 (2002) 117–124.
- [9] C. Lartigue, A. Le Bail, A. Pecheron-Guegan, *J. Less-Common Met.* 129 (1987) 181–186.